MODELING DME ADDITION EFFECTS TO FUEL ON PAHS AND SOOT IN LAMINAR COFLOW ETHYLENE/AIR DIFFUSION FLAMES USING TWO PAH MECHANISMS

F. Liu*, S. B. Dworkin,†, M. J. Thomson**, and G. J. Smallwood***
Fengshan.liu@nrc-cnrc.gc.ca
* Inst. for Chem. Process and Envir. Tech., National Research Council, Ottawa, ON., K1A 0R6
** Dept. of Mech. and Indust. Eng., University of Toronto, 5 King's College Road, Toronto, ON., M5S 3G8
† Now at Dept. of Mech. and Indust. Eng., Ryerson University, 35 Victoria St., Toronto, ON, Canada M5B 2K3

Abstract

Effects of dimethyl ether (DME) addition to fuel on polycyclic aromatic hydrocarbons (PAH) and soot formation in laminar coflow ethylene/air diffusion flames were revisited numerically. Numerical calculations were conducted using two gas-phase reaction mechanisms with PAH formation and growth: one is the C_2 chemistry of the Appel, Bockhorn, and Frenklach (ABF) mechanism with PAH growth up to A4 (pyrene), the other is also a C_2 chemistry mechanism newly developed at DLR (DLR) with PAH growth up to A5 (corannulene). Soot was modeled based on the assumptions that soot inception is due to the collision of two pyrene molecules, and soot surface growth follows a hydrogen abstraction carbon addition (HACA) sequence. The DLR mechanism predicted much higher concentrations of pyrene than the ABF mechanism. A much smaller value of α in the surface growth model associated with the DLR mechanism has to be used to predict the correct peak soot volume fraction. Both reaction mechanisms are capable of predicting the synergistic effect of DME addition to fuel on PAH formation. The locations of high PAH concentrations predicted by the DLR mechanism are in much better agreement with available experimental observations. A weak synergistic effect of DME addition on soot formation was predicted by the ABF mechanism. The DLR mechanism failed to predict the synergistic effect on soot. The likely causes for such a failure and the implications for future research on soot inception and surface growth are discussed.

Introduction

Combustion of oxygenated fuels is in general very clean in terms of particulate (soot) formation. There have been strong interests in blending oxygenated fuels to conventional hydrocarbon fuels to control soot formation. Dimethyl ether (DME) has received considerable research attention in recent years because it can be produced economically in large quantities.

Because of the complex nature of chemical kinetics, however, addition of a relatively small amount of DME to a conventional hydrocarbon fuel does not always lower soot formation. For example, it has been shown in several recent experimental studies conducted in laminar counterflow [1] and coflow ethylene/air diffusion flames [2,3] that addition of a small amount of DME to ethylene results in the so-called *synergistic* effect, i.e., PAHs and soot concentrations are actually enhanced to levels above those in the pure ethylene flame. Yoon et al. [1] and McEnally and Pfefferle [2] explained the synergistic effect of DME addition to ethylene on PAHs and soot formation by the enhanced methyl radical concentrations from the decomposition of DME, which then prompt propargyl formation and finally lead to increased benzene, PAHs, and soot through the self-combination reaction of propargyl. A recent numerical study conducted by Bennett et al. [4] provided numerical evidence to support the explanation suggested by Yoon et al. [1] and McEnally and Pfefferle

[2] and again emphasized the importance of the propargyl self-recombination reaction leading to benzene and to the synergistic effect. More recently, Liu et al. [3] conducted a more systematic study of the effects of DME addition to fuel in laminar coflow ethylene/air diffusion flames with the compositions of the fuel stream varying from pure ethylene to pure DME. The gas-phase reaction mechanism used by Liu et al. [3] was compiled based on the C_2 chemistry with a PAH mechanism (up to pyrene) of Appel et al. [5] (hereafter called the ABF mechanism) and DME 2000 [6]. Soot formation was modelled with a PAH based inception mechanism, i.e., collision of two pyrene molecules, and the HACA mechanism for surface growth and oxidation. The numerical results of Liu et al. qualitatively reproduced the synergistic effect of DME addition to ethylene, even the range of DME addition over which the synergistic effect occurs was reproduced. Although the synergistic effect on soot formation was also predicted by the model, the magnitude of the effect and the range of DME addition were significantly underpredicted. Through a detailed examination of reaction pathways leading to benzene formation in the numerical results calculated using the ABF mechanism, Liu et al. found that the synergistic effect on benzene formation was not caused by the self-recombination of propargyl, but mainly through the cyclization reactions of l-C_6H_6 and n-C_6H_7 [3].

Although the ABF mechanism was found somewhat successful in the prediction of the synergistic effects of DME addition to ethylene on PAHs and soot, it failed to predict the correct locations of high PAH concentrations, the correct magnitude of the synergistic effect on soot, and the correct levels of soot volume fraction in the flame centerline region. The latter has been a well known drawback of the current practice of soot formation modelling in laminar coflow ethylene diffusion flames. However, it is unclear if the failure to predict the correct soot levels in the flame centerline region is mainly due to deficiencies in the PAH formation mechanism or deficiencies in the soot formation model. In an attempt to overcome the potential deficiencies of the Appel et al. PAH formation mechanism revealed in soot formation modelling in the laminar ethylene diffusion flame, Dworkin et al. [7] conducted a numerical study of soot formation in a laminar coflow ethylene/air diffusion flame, which had been first studied by Santoro et al. [8], using a modified PAH formation mechanism based on the recent work of Slavinskaya and Frank [9] at DLR (hereafter called the DLR mechanism). The soot model used by Dworkin et al. [7] was essentially the same as that used by Liu et al. [3]. The only difference lies in the value of α, the fraction of reactive surface sites for soot particle surface growth. Dworkin et al. [7] showed that the DLR PAH mechanism predicted much higher soot volume fractions in the flame centerline region, to levels comparable to experimental data, though they are still about a factor of 2 to 3 lower. Nevertheless, the study of Dworkin et al. [7] demonstrated that the DLR PAH formation mechanism is promising to overcome the deficiencies of the ABF mechanism in modelling soot formation in the laminar ethylene diffusion flame.

It is important to understand the mechanism of the synergistic effect from the viewpoint of formation pathways leading to PAH and soot formation. The ability to predict the synergistic effect on PAH formation also serves as an important criterion to probe the validity of a PAH formation mechanism and/or soot formation model. With this in mind, the present study further investigated the performance of the DLR PAH mechanism in the prediction of the synergistic effects of DME addition to fuel on PAH and soot formation in a laminar coflow ethylene/air diffusion flame at atmospheric pressure. Numerical results obtained using the DLR mechanism are compared to those from the ABF mechanism and available experimental observations in the literature.

Numerical Model

Governing Equations, Soot and Radiation Models

The governing equations have been described in previous studies, e.g., [10], and will not be provided here. It suffices to mention that the steady-state fully-coupled elliptic conservation equations for mass, momentum, energy, and species mass fractions in axisymmetric cylindrical coordinates and in the low Mach number limit were solved.

The soot formation model has also been described in detail in [11]. Soot inception was assumed to be the result of collision of two A4 (pyrene) molecules. The subsequent surface growth and oxidation were assumed to follow the HACA mechanism [5]. It is important to point out that the value of the parameter α, which represents the fraction of reactive soot surface sites and lies in the range of 0 to 1, was revised when different PAH formation mechanisms were used as detailed in [7]. When the ABF mechanism was used, α was assumed as [11]

$$\alpha = \min[0.004 \exp(10800 / T), 1.0]. \quad (1)$$

which takes the value of unity for temperatures below about 1950 K, i.e., α takes the value of unity almost everywhere in soot formation regions of the flame. On the other hand, a much smaller value of α = 0.078 had to be used by Dworkin et al. [7] to predict the correct peak soot volume fraction in the Santoro flame. The much smaller value of α required in the study of Dworkin et al. [7] to match the expected peak soot volume fraction is associated with much higher soot inception rates, since the DLR mechanism predicted higher concentrations of A4 in the ethylene diffusion flame. As a result of the large difference in the values of α associated with the ABF and DLR mechanisms, it is expected that the relative contributions of inception and surface growth to the total soot mass will be different, i.e., surface growth dominates with the ABF mechanism and inception plays a greater role with the DLR mechanism.

The radiation model used here has also been well documented in the literature, e.g., [11 and references cited therein]. The radiative transfer equation in 2D axisymmetric cylindrical coordinates was solved by the discrete-ordinates method. The absorption coefficients of the combustion products CO, CO_2 and H_2O were obtained using a 9-band model. The absorption coefficient of soot was calculated using the Rayleigh expression.

Chemical Kinetic Mechanisms

Two gas-phase reaction mechanisms that include PAH formation were employed in this study. One is the ABF mechanism [5], which was primarily developed for C_2 hydrocarbons with PAH formation. The other one is the recently developed DLR mechanism [7,9]. The ABF mechanism contains 101 species and 544 reactions with PAH formation and growth up to A4. The DLR mechanism involves 94 species and 719 reactions with PAH formation and growth up to A5 (corannulene). Further details of the DLR mechanism have been discussed by Dworkin et al. [7]. It should be noted that the PAH reactions in the DLR mechanism are more numerous and comprehensive than in the ABF mechanism, where they comprise only a simple PAH HACA growth scheme.

For the purposes of this study, the ABF and DLR mechanisms were extended by adding the species and reactions related to DME combustion from a detailed DME mechanism [6], which contains 79 species. This was achieved by simply appending species and reactions from the DME mechanism that are not present in either the ABF or the DLR mechanisms. As a result, both the extended ABF and the extended DLR mechanism contain an additional 50 species and 241 reactions.

Results and Discussion

The laminar coflow diffusion flame burner consisted of a central fuel tube of 10.9 mm inner diameter (the fuel tube thickness was 0.94 mm) and a co-annular tube of 88 mm inner diameter for the air supply. The burner was operated at 1 atm. Air supply was maintained at a flow rate of 284 l/min. The total volumetric flow rate of the fuel stream containing a mixture

of ethylene and DME was also kept constant at 194 ml/min. Both fuel and air were delivered at room temperature. When a certain amount of DME (volume basis) was added to the fuel stream, the same amount (volume basis) of ethylene was reduced to keep the carbon mass flow rate constant. The composition of the fuel stream was parameterized using the ratio of the DME flow rate to the total fuel flow rate, i.e., $\beta = Q_{DME} / (Q_{DME} + Q_{C_2H_4})$. Numerical calculations were conducted for six values of β, i.e., β = 0, 0.0625, 0.125, 0.1875, 0.25, and 0.375. It is noted that β = 0 corresponds to the pure ethylene flame. The numerical methods, inlet and boundary conditions, computational domain, and mesh resolution were described in detail in [3]. Unless otherwise indicated all the results of the DLR mechanism were obtained with α = 0.078.

Soot Volume Fraction Distributions

The predicted soot volume fraction distributions in the six flames using the ABF and the DLR mechanisms are shown in Figs. 1 and 2, respectively. The peak soot volume fraction and the peak centerline soot volume fraction in each case are also indicated in the figure (with the centerline peak soot volume fraction appearing just below the peak soot volume fraction).

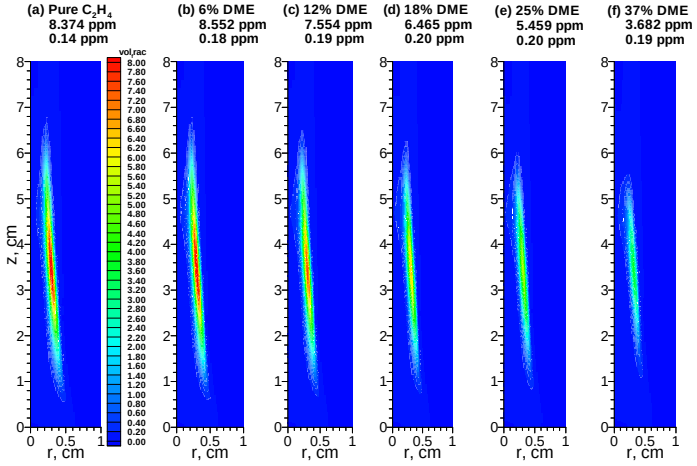

Fig. 1 Distributions of soot volume fraction calculated using the ABF mechanism.

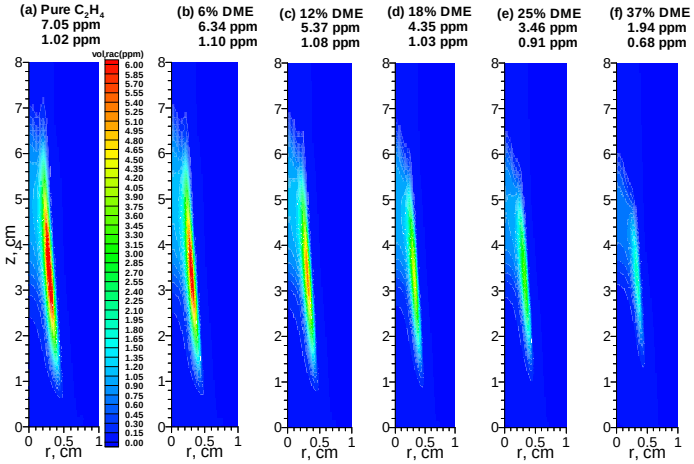

Fig. 2 Distributions of soot volume fraction calculated using the DLR mechanism.

Three observations can be made from these two figures. First, there is a synergistic effect on peak soot volume fraction when a relatively small amount of DME (up to 12%) is added to ethylene when the ABF mechanism is used, Fig. 1. However, there is no synergistic effect on

peak soot volume fraction when the DLR mechanism is used, Fig. 2. The second observation is that the DLR mechanism predicts significantly higher soot volume fractions in the flame centerline region with peak centerline values just over 1 ppm for Flames a, b, c, and d in Fig. 2, while the ABF mechanism predicts that soot volume fractions are very low in the flame centerline region (centerline values remain below 0.2 ppm for all the six flames in Fig. 1). It is noticed that there is a synergistic effect on soot along the flame centerline in both the ABF and DLR results, especially the latter. Thirdly, the peak soot volume fraction in the pure ethylene flame of about 8.4 ppm predicted by the ABF mechanism is in better agreement with available experiment in the literature. Using the α value of 0.078 employed by Dworkin et al. [7] in the calculation of the Santoro flame, where the visible flame height was about 88 mm and the peak soot volume fraction is about 10 ppm due to a higher fuel flow rate than that in the present study, resulted in a peak soot volume fraction of about 7 ppm in the pure ethylene flame ($\beta = 0$). The experimentally measured peak soot volume fraction in the ethylene flame studied here is about 8 ppm and the visible flame height is about 64 mm [12]. The different performance of $\alpha = 0.078$ in the modelling of soot in the Santoro flame by Dworkin et al. [7] and the present smaller ethylene flame suggests that the optimal α associated with the DLR mechanism might depend on certain parameters, such as temperature and soot particle diameter. These parameters are in turn altered by conditions under which the flame is established, including but not limited to the fuel flowrate, the type of fuel, and the amount and type of additive.

Besides the difference in the value of α associated with the ABF and the DLR mechanisms, another difference between them lies in their temperature dependence. The α associated with the ABF mechanism has weak temperature dependence as given in Eq. (1), while the α used in the DLR mechanism is independent of temperature. To assess the potential effect of neglecting the temperature dependence of α on the calculated soot volume fraction with the DLR mechanism, two additional runs were carried out in which the value of α was calculated as

$$\alpha = \min[0.078 \times 0.004 \exp(10800 / T), 0.078] \quad . \tag{2}$$

A comparison between the results using Eq. (2) and those using a constant α of 0.078 shows that the soot volume fractions remain essentially the same (the differences remain below 3%), and there is still no synergistic effect on soot volume fraction.

For the purpose of finding the optimal value of α associated with the DLR mechanism that reproduces the peak experimental soot volume fraction in the present pure ethylene flame, additional calculations were also conducted using different values of α. It was found that $\alpha = 0.09$ yields a peak soot volume fraction of 8.3 ppm, which is in good agreement with the experimental data of about 8 ppm and is almost identical to that calculated with the ABF mechanism using α given in Eq. (1). Therefore, $\alpha = 0.09$ is regarded as the optimal value in terms of the peak soot volume fraction for the present flame.

Mole Fraction of Pyrene and Benzene

Pyrene is very important in the present context for two reasons. First, it is a four-ring PAH. Secondly, it is critical to soot formation, since it is the assumed PAH species responsible for soot inception in the soot model. The predicted pyrene (A4) mole fraction distributions by the ABF and the DLR mechanisms are shown in Figs. 3 and 4, respectively, with the peak value in each flame indicated. In the results of the ABF mechanism, the A4 mole fraction peaks at 6% DME addition (Fig. 3(b)). However, the maximum A4 mole fraction occurs at 25% DME addition when the DLR mechanism is used (Fig. 4(e)). It is also apparent that the A4 mole fractions are about a factor 5 to 6 times higher when the DLR mechanism is used. It is therefore expected that the soot inception rates are much higher in the DLR results.

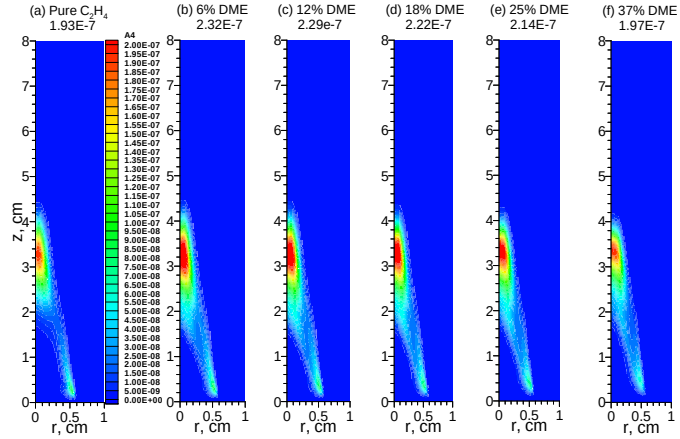

Fig. 3 Distributions of pyrene mole fraction calculated by the ABF mechanism.

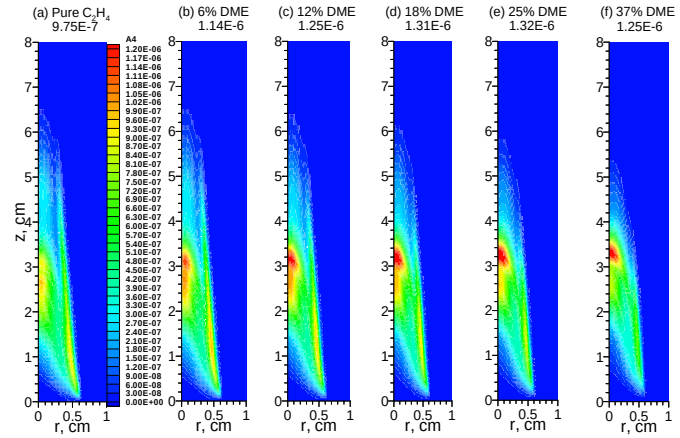

Fig. 4 Distributions of pyrene mole fraction calculated by the DLR mechanism.

To reveal the relative importance of soot inception and surface growth to soot volume fraction in different regions of the flame, namely the centerline and the wing (outer annular region exhibiting the peak soot volume fraction at a given height) in the results of the DLR mechanism, additional calculations were conducted for Flames a and b with the soot surface growth process turned off by setting $\alpha = 0$. The soot volume fraction distributions without surface growth for Flames a and b are shown in Fig. 5. It is noticed that the flames emit soot. This is because soot oxidation by O_2 is also removed when soot surface growth is turned off by setting $\alpha = 0$ in the HACA soot surface growth sequence [5] and soot oxidation by OH is insufficient to fully consume soot. Fig. 5 shows that the peak soot volume fraction reaches 0.67 and 0.71 ppm in the pure ethylene flame and the flame with 6% DME addition, respectively, due to inception alone. Although the highest soot volume fractions are not in the flame centerline region, the high centerline soot volume fractions are close to the peak vaues. A comparison between Figs. 5 and 2 indicates that soot inception contributes about 70% to soot volume fraction in the centerline region in the results of the DLR mechanism. However, the contribution of soot inception in the flame wing is still much smaller (less than 10%) even in the results of the DLR mechanism, which predicts much higher pyrene concentrations than the ABF mechanism as shown in Figs. 3 and 4. The majority of soot along the flame wing is produced through the surface growth process. The enhanced soot volume fractions with the addition of 6% DME shown in Fig. 5 are expected from the enhanced pyrene mole fractions shown in Fig. 4.

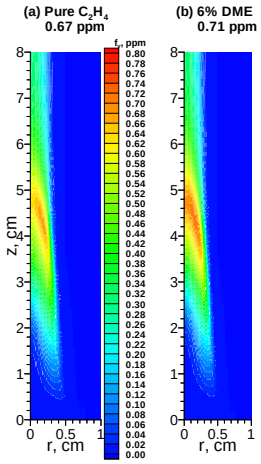

Fig. 5 Distributions of soot volume fraction calculated using the DLR mechanism without soot surface growth and oxidation by setting $\alpha = 0$.

Distributions of A1 (benzene) mole fraction calculated using the ABF and DLR mechanisms are shown in Figs. 6 and 7, respectively. The peak value in each flame is also indicated. It is seen that both mechanisms predicted a similar magnitude of the synergistic effect at about 45%, which is the relative increase in the A1 mole fraction in Flame b (6% DME addition) over Flame a (pure ethylene flame). The maximum A1 mole fraction occurs at 6% DME addition when ABF is used, Fig. 6, while the maximum value occurs at 12% DME addition with the DLR mechanism, Fig. 7, though the A1 mole fractions in Flame c are only slightly higher than those in Flame b. Results of the DLR mechanism are in better agreement with the PLIF images reported in [3], where the signal intensities of Flame c (12% DME addition) are also slightly higher than those of Flame b, assuming A1 contributes the most to the PLIF signals due to its much higher concentrations than larger PAH species. In addition, the locations of high A1 concentrations predicted by the DLR mechanism are lower than those in the ABF results (around z = 1.75 cm vs. around z = 2.5 cm). Again, the locations of high benzene concentrations are in better agreement with the PLIF images reported in Ref. [3], where the high single intensities in the centreline region occur around z = 1.5 cm.

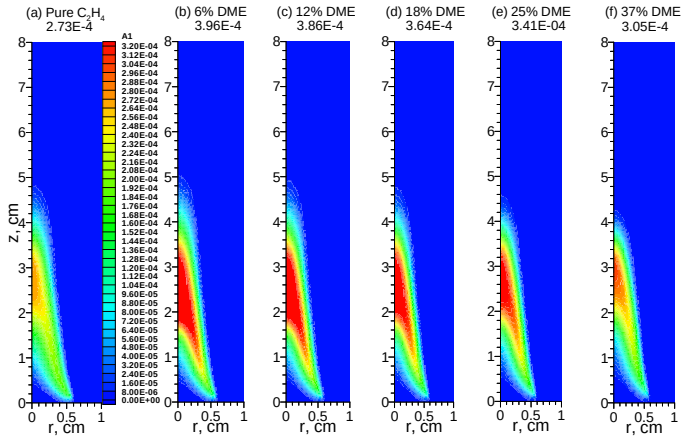

Fig. 6 Distributions of benzene mole fraction calculated using the ABF mechanism.

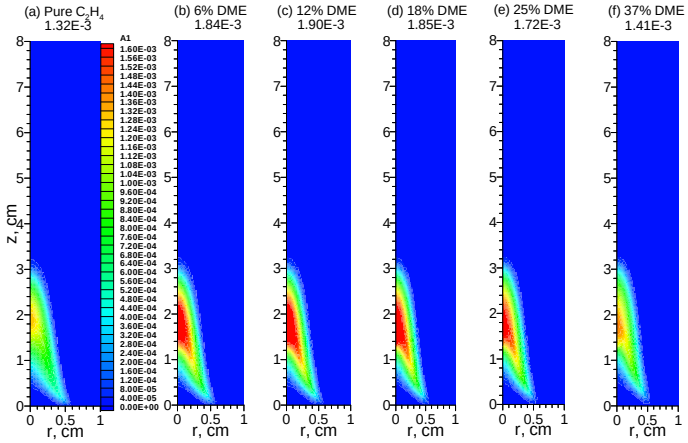

Fig. 7 Distributions of benzene mole fraction calculated using the DLR mechanism.

To better demonstrate the synergistic effect of DME addition on A1 and A4 formation, the normalized peak mole fractions (by the respective value in the pure ethylene flame) of A1 and A4 are shown in Fig. 8. Overall, the ABF and DLR mechanisms predicted similar synergistic effects of DME addition on A1, albeit the high A1 concentrations appear earlier in the flame centerline regions with the DLR mechanism, which agree with the experimental observations [3]. The much stronger synergistic effect on A4 formation predicted by the DLR mechanism, Fig. 8, is expected since the DLR mechanism included additional PAH growth pathways involving methyl and propargyl [7,9] that are absent in the ABF mechanism.

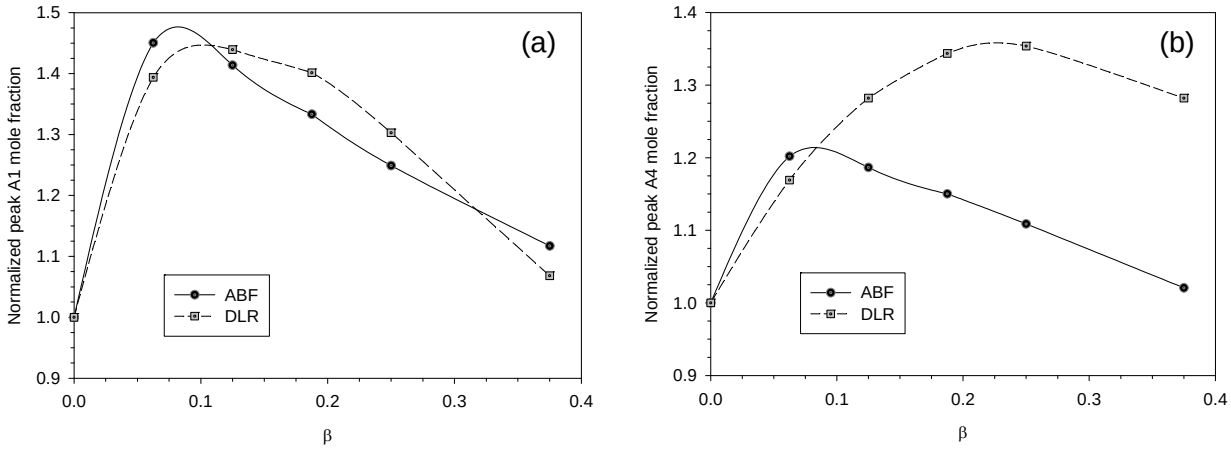

Fig. 8 Variations of the normalized peak mole fractions of (a) A1 and (b) A4 with the amount of DME addition to the fuel stream.

Mole Fraction of Acetylene

Acetylene plays an even more important role in soot loading, since it is the primary soot surface growth species and the majority of soot mass is from the surface growth process. This point has been well established in previous soot studies in the literature and it is shown earlier in this study, compare Figs. 2 and 5. The predicted acetylene mole fraction distributions are shown in Figs. 9 and 10 with the ABF and DLR mechanism, respectively.

Although the mole fractions of acetylene predicted by the ABF and the DLR mechanism are very similar, there are two main differences. First, the synergistic effect of DME addition on C_2H_2 is slightly stronger in the results of the ABF mechanism. Secondly, C_2H_2 survives longer in the centerline region, i.e., it disappears at a higher flame height, in the results of the ABF mechanism, which is consistent with the higher locations of high benzene concentrations. This implies that there are longer residence times for soot surface growth

when the ABF mechanism is used. These higher C_2H_2 concentrations (and stronger soot synergy) seen with the ABF mechanism seem to support the hypothesis that DME addition on soot synergy may be more strongly related to surface growth than to inception along the wings of the flame. This results is in contrast to the explanations offered by Yoon et al. [1] and McEnally and Pfefferle [2] that the synergistic effect on soot is PAH related. A direct comparison between the results shown in Figs. 2 and 5 obtained with the DLR mechanism indeed supports the conjecture that soot surface growth is dominant along the flame wings.

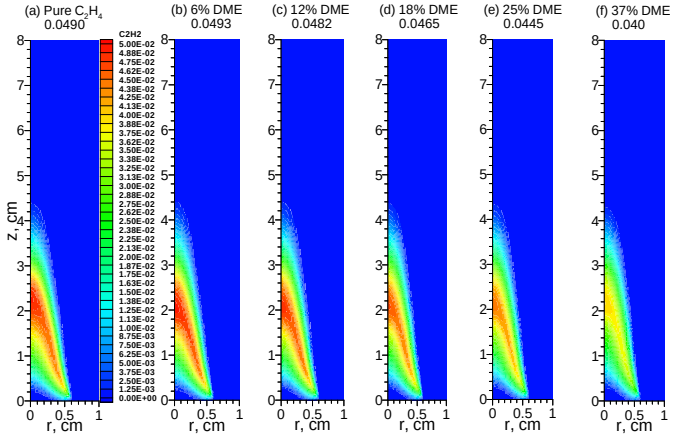

Fig. 9 Distributions of acetylene mole fraction predicted by the ABF mechanism.

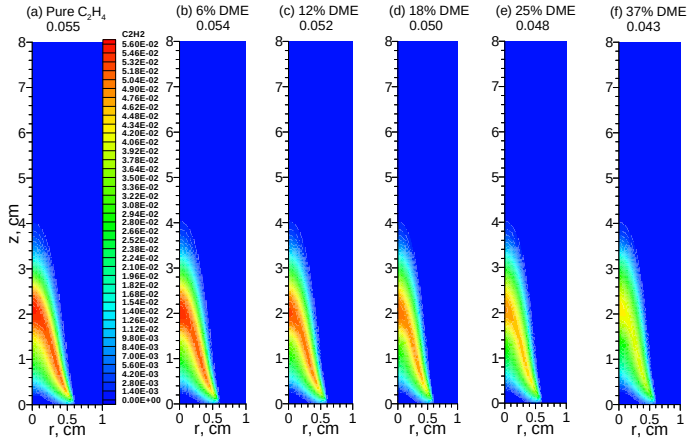

Fig. 10 Distributions of acetylene mole fraction predicted by the DLR mechanism.

Conclusions

The effects of DME addition to fuel on PAH and soot formation in a laminar ethylene/air diffusion flame were numerically investigated by employing two gas-phase reaction mechanisms and a PAH-based soot formation model. The results indicated that both the ABF and the DLR mechanisms are capable of predicting the experimentally observed synergistic effect of DME addition on PAH formation. When the ABF mechanism was used, the predicted soot volume fraction displays the synergistic effect on the wings of the flame with a relatively small amount of DME addition (at 6% and 12%), though the effect is weaker than the experimental observation. When the DLR mechanism is used, however, the predicted soot volume fraction fails to display the synergistic effect on the wings of the flame, though shows the effect on the flame centerline due to enhanced soot inception. The DLR mechanism predicted much higher A4 concentrations, by a factor of about 5 to 6, than the ABF mechanism. Although both mechanisms predicted a similar synergistic effect on A1 mole fraction, the locations of high A1 concentrations predicted by the DLR mechanism are in

much better agreement with available experimental observations. Both mechanisms predicted a weak synergistic effect of a small amount of DME addition on acetylene. The likely reason for the failure of the DLR mechanism to predict the synergistic effect on soot formation along the flame wings lies in the weaker contribution of surface growth to soot loading due primarily to the much smaller value of α and, to a lesser degree, the shorter residence time of the soot surface growth process associated with the earlier disappearance of acetylene. Since both mechanisms predicted comparable levels of PAH synergy, and soot synergy along the centerline (where soot formation is inception dominated), and the ABF mechanism predicted stronger acetylene synergy and soot synergy along the wings (where soot formation is acetylene/surface growth dominated), it is likely the case that the synergistic effect is not completely explained by a methyl-propargyl-PAH route, but rather also involves acetylene. If the synergistic effect were only attributable to the methyl-propargyl-PAH route as suggested by Yoon et al. [1] and McEnally and Pfefferle [2], then a synergestic effect along the wings of the flame with the DLR mechanism would have been seen, since synergy was strong with A1 and A4.

Acknowledgements
The authors acknowledge Dr. Nadezhda A. Slavinskaya of the German Aerospace Centre (DLR) for providing the DLR reaction mechanism. Computations were performed on the GPC supercomputer at the SciNet HPC Consortium. SciNet is funded by: the Canada Foundation for Innovation under the auspices of Compute Canada; the Government of Ontario; Ontario Research Fund - Research Excellence; and the University of Toronto. The authors from the University of Toronto acknowledge NSERC for financial support.

References
[1] Yoon, S.S., Anh, D.H., Chung, S.H., “Synergistic effect of mixing dimethyl ether with methane, ethane, propane, and ethylene fuels on polycyclic aromatic hydrocarbon and soot formation”, *Combust. Flame* 154: 368-377 (2008).
[2] McEnally, C.S., Pfefferle, L.D., “The effects of dimethyl ether and ethanol on benzene and soot formation in ethylene nonpremixed flames”, *Proc. Combust. Inst.* 31: 603-610 (2007).
[3] Liu, F., He, X., Ma, X., Zhang, Q., Thomson, M.J., Guo, H., Smallwood, G.J., Shuai, S., Wang, J., “An experimental and numerical study of the effects of dimethyl ether addition to fuel on polycyclic aromatic hydrocarbon and soot formation in laminar coflow ethylene/air diffusion flames”, *Combust. Flame* 158: 547-563 (2011).
[4] Bennett, B.A., McEnally, C.S., Pfefferle, L.D., Smooke, M.D., Colket, M.B., “Computational and experimental study of the effects of adding dimethyl ether and ethanol to nonpremixed ethylene/air flames”, *Combust. Flame* 156: 1289-1302 (2009).
[5] Appel, J., Bockhorn, H., Frenklach, M., “Kinetic modeling of soot formation with detailed chemistry and physics: laminar premixed flames of C2 hydrocarbons”, *Combust. Flame* 121: 122-136 (2000).
[6] Kaiser, E.W., Wallington, T.J., Hurley, M.D., Platz, J., Curran, H.J., Pitz, W.J., Westbrook, C.K., “Experimental and modeling study of premixed atmospheric-pressure dimethyl ether-air flames”, *J. Phys. Chem. A* 104: 8194-8206 (2000).
[7] Dworkin, S.B., Zhang, Q., Thomson, M.J., Slavinskaya, N.A., Riedel, U., “Application of an enhanced PAH growth model to soot formation in a laminar coflow ethylene/air diffusion flame”, Combust. Flame, (2011) in press, (doi:10.1016/ j.combustflame.2011.01.013).
[8] Santoro, R.J., Semerjian H.G., Dobbins, R.A., “Soot particle measurements in diffusion flames”, Commbust. Flame 51: 203-218 (1983).

[9] Slavinskaya, N.A., Frank, P., “A modelling study of aromatic soot precursors formation in laminar methane and ethene flames,” *Combust. Flame* 156: 1705-1722 (2009).
[10] Guo, H., Liu, F., Smallwood, G.J., Gülder, Ö.L., “Numerical study on the influence of hydrogen addition on soot formation in a laminar ethylene-air diffusion flame”, *Combust. Flame* 145: 324-338 (2006).
[11] Zhang, Q., Guo, H., Liu, F., Smallwood, G.J., Thomson, M.J., “Modeling of soot aggregate formation and size distribution in a laminar ethylene/air coflow diffusion flame with detailed PAH chemistry and an advanced sectional aerosol dynamics model, *Proc. Combust. Inst*. 32: 761-768 (2009).
[12] Liu, F., Guo, H., Smallwood, G.J., Gülder, Ö.L., “Effects of gas and soot radiation on soot formation in a coflow laminar ethylene diffusion flame”, *JQSRT* 73: 409-421 (2002).